

Synthesis and photoluminescent properties of SnO-containing germanate and germanosilicate glasses

A. I. Chernov¹ · B. I. Denker¹ · R. P. Ermakov^{1,2} · B. I. Galagan¹ ·
L. D. Iskhakova² · S. E. Sverchkov¹ · V. V. Velmiskin² · E. M. Dianov²

Received: 6 April 2016 / Accepted: 24 August 2016 / Published online: 1 September 2016
© Springer-Verlag Berlin Heidelberg 2016

Abstract Divalent tin-containing germanate glasses have demonstrated wide photoluminescence similar to that of tin silicate glasses discovered recently. In comparison with silicate glasses, the germanate glasses are characterized by longer emission lifetimes ($145 \div 440 \mu\text{s}$), emission peaking at $1.59 \div 1.64 \mu\text{m}$ and the absence of SnO disproportionation into SnO_2 and Sn during glass synthesis. The potential fabrication of optical fiber via the $\text{SnC}_2\text{O}_4 + \text{GeO}_2$ powder in silica tube method was demonstrated.

1 Introduction

Some 5p and 6p elements (bismuth first of all, but also Pb, Te, etc.) can form infrared-emitting centers in oxide glasses synthesized under reducing conditions [1–3]. Such activated glasses are promising materials for tunable fiber lasers and wideband amplifiers.

Our recent paper [4] described the wideband near-infrared photoluminescence in divalent tin-containing silicate glass. This infrared emission had many attractive characteristics for laser and telecommunication applications, similar to those of bismuth-activated glasses and fibers. But SnO– SiO_2 glass is very difficult from technological point of view. The main difficulty in this glass synthesis is the partial disproportionation of SnO into SnO_2 and metallic tin, both insoluble in the glass melt. We have tried to overcome

this difficulty by total or partial substitution of SiO_2 by GeO_2 as a more fusible oxide. We knew [5] that SnO– GeO_2 glasses do exist, but we have found no data about the vitrification field in this system. Therefore, the goals of the present paper were the following:

- To synthesize SnO– GeO_2 and also some SnO– GeO_2 – SiO_2 glass samples with different ratios of the components. To outline the glass forming region and the required synthesis conditions.
- To investigate the photoluminescence properties of the synthesized samples (if any). Our interest was aimed at the long-lasting photoluminescence within the fiber telecommunication window ($\sim 1300 \div 1700 \text{ nm}$).
- To study a potential of optical fiber fabrication of SnO-containing germanate glass.

2 Glass samples preparation

For the preparation of SnO– GeO_2 glasses in nonoxidizing conditions, we have developed a special procedure. The starting material for the synthesis was the mixture of GeO_2 (99.999 wt% purity) and stannous oxalate SnC_2O_4 (Sigma Aldridge CAS: 814-94-8). The proper choice of the suitable crucible material for this glass is very important. Our preliminary tests have shown that iridium rapidly degrades in the SnO– GeO_2 melt. High-purity silica glass or silica ceramic crucibles are possible materials, but the crucible walls are seriously attacked by the melt and the resulting glass becomes enriched with SiO_2 . That is why in case of purely germanate glasses we have preferred to use alumina ceramic crucibles.

The synthesis was held in a hermetic chamber in dry nitrogen atmosphere to prevent SnO oxidation to SnO_2 . A

✉ B. I. Denker
denker@Lst.gpi.ru

¹ A. M. Prokhorov General Physics Institute of RAS, Vavilov Str. 38, Moscow, Russia 119991

² Fiber Optics Research Center of RAS, Vavilov Str. 38, Moscow, Russia 119991

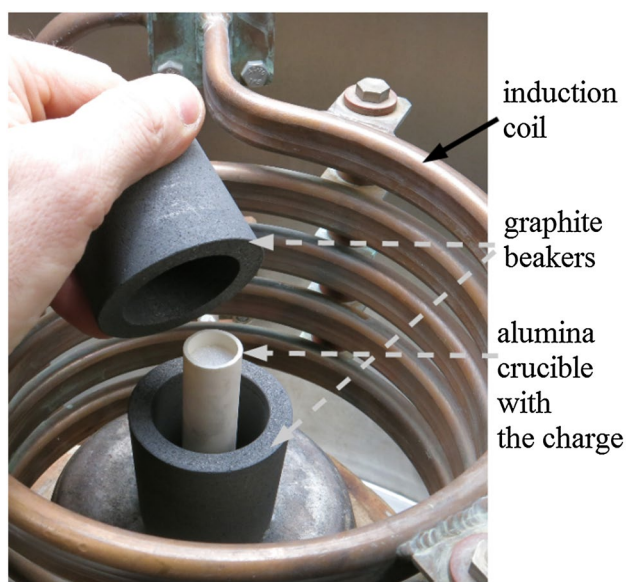


Fig. 1 Photograph of the thermal unit

couple of graphite beakers in high frequency coil served as a heating source as shown in Fig. 1. The crucible with the charge of $\text{SnC}_2\text{O}_4\text{-GeO}_2$ mixture was placed inside the beakers.

About 15 g of a $\text{GeO}_2\text{-SnC}_2\text{O}_4$ mixture was slowly heated in the crucible to a temperature of ~ 400 °C for thermal decomposition of stannous oxalate: $\text{SnC}_2\text{O}_4 = \text{SnO} + \text{CO} + \text{CO}_2$. Then, the temperature was raised to $1200 \div 1600$ °C (depending on the SnO/GeO_2 ratio) and kept for 30 min. After switching the power off and cooling the thermal unit down to room temperature, the crucible contained transparent glass that could be extracted by crucible destruction. In contrast to tin silicate glasses, all the tin germanate glasses showed no tin disproportionation: The glasses had no metallic tin or any SnO_2 inclusions. The samples had some striae that seem inevitable in non-stirred glass. A set of glasses with variable SnO content was prepared. The SnO percentage in the charge was varied from 0 to 50 %mol. The attempt to prepare a sample with 60 %mol SnO failed—the melt crystallized.

We have also prepared a few samples of $\text{SnO-GeO}_2\text{-SiO}_2$ and SnO-SiO_2 charges.

Preparation of such samples was done in two stages. At the first stage, about 100 g of 50SnO-50SiO_2 mixture was melted in a silica ceramic crucible. The obtained glass was covered by a SnO_2 crust and had metal Sn droplet inclusions due to SnO disproportionation. After crashing this glass into small crumbs, the pieces with no visible inclusions were selected, grinded and mixed with additional SiO_2 or GeO_2 . At the second stage, this mixture was melted in the same way as the previous samples in alumina ceramic crucibles.

Table 1 presents the list of successfully prepared glass samples. The sample #11 with charge composition 50SnO-50GeO_2 was prepared in the same way as all the other tin germanate glasses, but using silica glass crucible instead of alumina one.

Polished plates of 3.5 mm thickness were fabricated of all of the prepared glasses.

3 Glass samples investigation

The following investigations were fulfilled with the samples:

- X-ray spectrometry analysis for composition control;
- optical transmission in 200–2000 nm spectral range;
- photoluminescence spectra in 850–2200 nm range;
- photoluminescence decay kinetics.

The main results of these investigations are summarized in Table 1.

3.1 The energy-dispersive X-ray spectroscopy (EDX) analysis

The elemental analysis was performed with JSM-5910LV (JEOL) scanning electron microscope instrumented by X-ray energy-dispersive (EDX) analysis AZtecENERGY (Oxford Instruments) analytical system. The analysis results are summarized in Table 1. It was detected that the samples prepared in alumina crucibles can contain a few %mol of alumina. Leaping ahead, we should state we have found no correlation of the luminescent properties with this impurity.

Sample #11 has identic charge composition to sample #8, but since it was prepared in silica glass crucible, the resulting glass contained more than 25 %mol. SiO_2 . It is interesting to note that despite high SiO_2 content, this sample was free of SnO_2 and metallic Sn inclusions. We have used this happenstance to make a clear glass when fabricating an optical fiber with $\text{SnO-GeO}_2\text{-SiO}_2$ core in a silica cladding (see below).

3.2 The optical transmission measurements

The transmission spectra of all prepared 3.5 mm thickness samples were measured in 200–2000 nm spectral range. Figure 2 demonstrates the transmission spectra of tin germanate sample set in the range 200–1000 nm.

It is clearly seen that the transparency region of SnO-GeO_2 glasses is a function of tin content: the higher the tin percentage—the narrower the transparency band. No additional absorption bands were detected in any of the 3.5-mm samples in their transmission ranges.

Table 1 List of the synthesized glass samples and some of their properties

Sample number	Charge content (%mol)	Analytic composition (%mol) ^a	Synthesis condition	Peak position of emission band (μm)	e-fold decay time (μs)	Comments
1	100GeO ₂	95GeO ₂ –5Al ₂ O ₃	Alumina crucible 1600 °C	No emission	–	
2	97.5GeO ₂ –2.5SnO	98.8GeO ₂ –1.2SnO	Alumina crucible 1580 °C	1.63	440	
3	95GeO ₂ –5SnO	95GeO ₂ –4.3SnO–0.7Al ₂ O ₃	Alumina crucible 1560 °C	1.64	412	
4	90GeO ₂ –10SnO	–	Alumina crucible 1580 °C	1.64	285	
5	80GeO ₂ –20SnO	71.7GeO ₂ –23.2SnO– 5.1Al ₂ O ₃	Alumina crucible 1440 °C	1.63	240	
6	70GeO ₂ –30SnO	–	Alumina crucible 1280 °C	1.59	170	
7	60GeO ₂ –40SnO	56.7GeO ₂ –34.1SnO– 9.2Al ₂ O ₃	Alumina crucible 1280 °C	1.60	150	
8	50GeO ₂ –50SnO	52.9GeO ₂ –40.7SnO– 6.4Al ₂ O ₃	Alumina crucible 1200 °C	1.59	145	
9	80SiO ₂ –20SnO	84.2SiO ₂ –15.8SnO	Alumina crucible 1640 °C	1.51	120	2-stage synthesis
10	39SnO–52SiO ₂ – 9GeO ₂	45.9SnO–48.5SiO ₂ – 5.6GeO ₂	Alumina crucible 1200 °C	1.52	80	2-stage synthesis
11	50GeO ₂ –50SnO	36.1GeO ₂ –25.5SiO ₂ – 38.4SnO	Silica crucible 1200 °C	1.60	120	1-stage synthesis

^a The analytic composition of the samples was measured in 3 ÷ 5 points across the polished samples. The Table presents averaged values

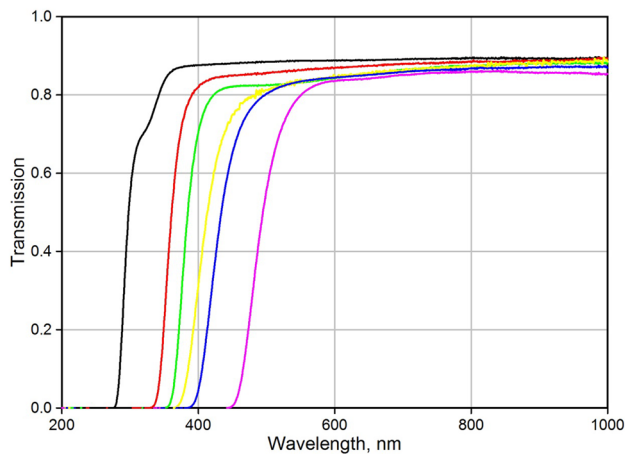


Fig. 2 Transmission spectra of 3.5 mm SnO–GeO₂ glass samples. Curves' sequence from *left to right* corresponds to glass sample set #1–#7 from Table 1 (except #6)

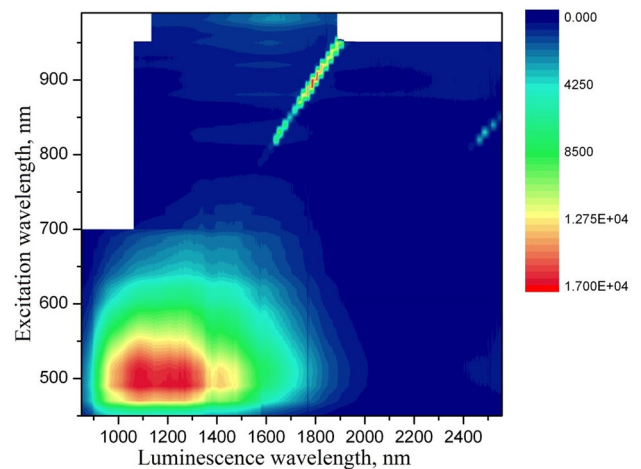


Fig. 3 Contour plot of photoluminescence intensity of the sample #11

3.3 Luminescent properties of the prepared glasses

All the synthesized tin-containing glasses showed infrared photoluminescence, while the tin free GeO₂ glass (control sample #1) prepared in the same highly reducing conditions showed no luminescence. Thus, it can be concluded

that all the emission centers are surely associated with tin. The overview photoluminescence excitation and emission spectral properties are presented by a contour plot in Fig. 3 for the sample #11. These measurements have been taken with a Horiba Jobin–Yvon NanoLog-4 system supplied with liquid nitrogen cooled InGaAs CCD detectors

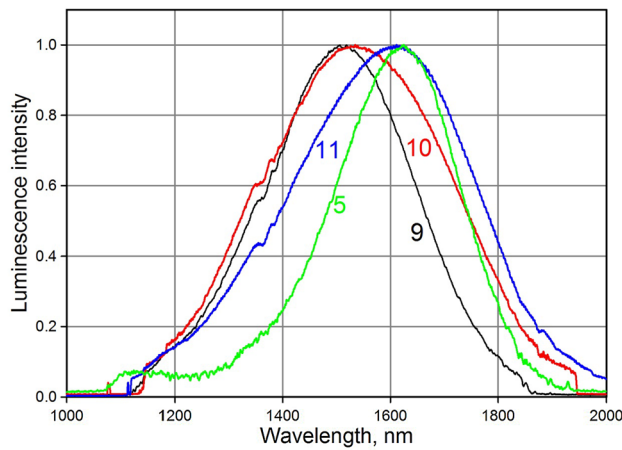


Fig. 4 Emission spectra of the selected glass samples from Table 1 under 0.955 μm excitation. Curve numbers coincide with sample numbers in the Table

working in spectral ranges 850–1550 and 1050–2200 nm. Photoluminescence excitation was made by a Xe lamp. Photoluminescence excitation mapping was performed with a 10-nm step in excitation.

The plot demonstrates a very wide (900–1800 nm) emission area. It is clearly seen that this emission is excited at about the edge of the glass sample transmission (~ 500 nm) and looks much more intensive than the ~ 1600 -nm emission band excited by 900 \div 1000 nm radiation. The latter looks very weak when measured with the mentioned device. Nevertheless, our interest was focused mostly at this band. The reason is the following. The ~ 1600 -nm emission decay function was more or less exponential with e-fold lifetimes measured in hundreds of μs . And when the glasses were excited near their absorption edge the luminescence decay kinetic functions were highly non-exponential while the e-fold lifetimes were in the order of a few μs only.

Therefore, our purpose was to explore the long-lifetime emission properties on the glass composition. For measuring the emission spectra, the samples were excited by the 3 W 955 nm laser diode modulated at 333 Hz. We used 600 grooves/mm grating monochromator and a dual-stage TEC cooled 2.6 μm cut-off InGaAs photodiode behind the 2.4-mm-thick silicon plate. The emission signal was detected by Signal Recovery noise-rejecting voltmeter 7310.

All the silica-free tin germanate glasses showed similar emission bands peaking at 1.59 \div 1.64 μm (an example is presented by curve 5 in Fig. 4).

The tin silicate glass showed, in accordance with [4], the emission band peaking at ~ 1.5 μm (curve 9 in Fig. 4). The ternary SnO–GeO₂–SiO₂ glasses (curves 10 and 11 in Fig. 4) demonstrate somewhat close to superposition of the curves 9 and 5.

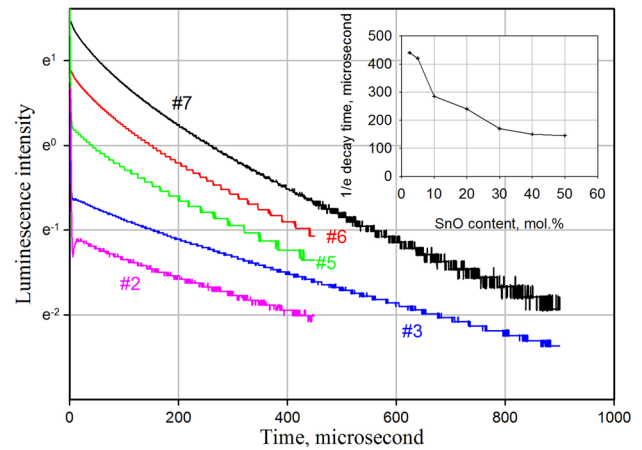


Fig. 5 Examples of emission decay curves in SnO–GeO₂ glasses. Curves from top to bottom correspond to sample sequence—#7, #6, #5, #3, #2. Insertion—e-fold lifetimes versus SnO percentage in the charge

The luminescence decay functions were recorded using a pulsed (pulse duration 7 ns) optical parametric oscillator tuned to 955 nm and the same InGaAs photodiode behind an IR filter. The filter transmitted wavelengths longer than 1.3 μm . The luminescence decay kinetics of the tin germanate glass sample concentration series are presented in Fig. 5. Since the geometry of the samples as well as that of the registration scheme was fixed, the initial amplitudes in Fig. 5 can be considered proportional to the amount of emission centers in the glass samples.

It can be seen that the photoluminescence amplitudes surely increase with tin content. On the other hand, at low tin content the decay function becomes close to exponential with the e-fold lifetime exceeding 400 μs . The insert in Fig. 5 is the plot of e-fold decay time versus SnO percentage. At low SnO concentration (sample #2), the lifetime reaches 440 μs . It should also be noted that the e-fold lifetime in tin germanate glasses is several times longer than that in tin silicate glass with similar tin content (samples #5 and #9, respectively).

The observed wideband photoluminescence with long decay time may be suitable for creating a new material for tunable lasers though the nature of the emission centers is not understood. It seems only clear that the formation of the emission centers requires oxygen deficiencies, same as in bismuth-activated glasses and laser fibers. Surely the concentration of the emission centers is very small since we were not able to detect their extinction. We have tried to estimate the order of magnitude for the extinction of the active centers by the following procedure. We have compared the photon fluxes emitted by sample #5 and by the plate of Yb–Er laser glass of the same thickness. Yb–Er laser glass has high (>80 %) luminescence quantum yield,

and the OPO pulse ($\lambda = 955 \mu\text{m}$) was practically 100 % absorbed in it. The luminescent responses of the two samples were integrated and compared. It turned out that the luminescent photons flux from Yb–Er laser glass was about 10^4 times higher than that in the tin germanate glass sample. In another words, only about 10^{-4} of the incident light was absorbed by the emission centers in the 3.5-mm-thick SnO–GeO₂ glass plate. The efficient absorption requires sample thickness $>20 \text{ m}$ which seems possible in fiber configuration only. Similar situation takes place in bismuth-activated fiber lasers [1], where the concentration of active centers should be also small and the active fiber lengths are measured in tens of meters.

4 Fabrication of optical fiber with a tin-containing core in silica cladding

During the present investigations, we have uncovered a promising method for the fabrication of clear silica-based glass samples, by melting a SnC₂O₄–GeO₂ mixture in silica glass containers. The glass prepared in this way had no SnO₂ or metal Sn inclusions, and the analysis showed that the obtained glass is SiO₂ enriched. For this reason, we can propose an original way to fabricate an optical fiber with a divalent tin-activated core.

The developed process of optical fiber fabrication consists of two stages. In the first stage, the 70SnC₂O₄–30GeO₂ mixture was heated in a flow of pure and dry Ar at the temperature of 400 °C. In these conditions, stannous oxalate decomposes as follows: $\text{SnC}_2\text{O}_4 \rightarrow \text{SnO} + \text{CO}\uparrow + \text{CO}_2\uparrow$. Then, the charge was placed in the Heraeus Suprasil F300 silica tube having the length of 120 mm, the outer and inner diameters 9 and 3 mm, respectively, which was initially tightly sealed from one end.

With the goal of melting this mixture, the tube was fixed in a feeding mechanism of drawing tower and filled with ultra-pure argon and passed through a furnace hot zone at the temperature of 1300 °C. In this process, the molten mixture formed the core, and the support tube formed the undoped silica cladding of the fiber preform. From this preform, the intermediate rods with length of 400 mm and diameter of 1 mm were drawn at 1840 °C.

In the second stage, the highest quality piece was selected from the obtained rods and was jacketed with the F300 tube with length of 150 mm and outer diameter of 9 mm. The multimode optical fiber with polymer protection coating was drawn from the fabricated preform at 1820 °C. Its length was about 20 m with an outer diameter of 120 μm and a core diameter of 10 μm . Figure 6 shows an electron microscope image of a cleaved fiber end.

It is seen that the cleavage is free of any defects and that the core has accurate round or slightly elliptical shape.

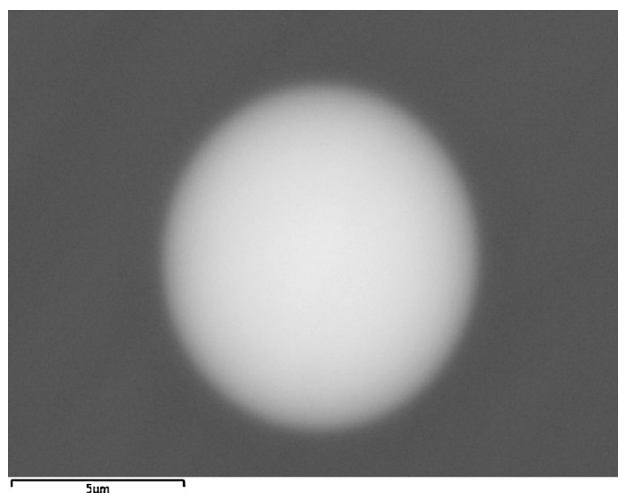


Fig. 6 Electron microscope image of a cleaved fiber end

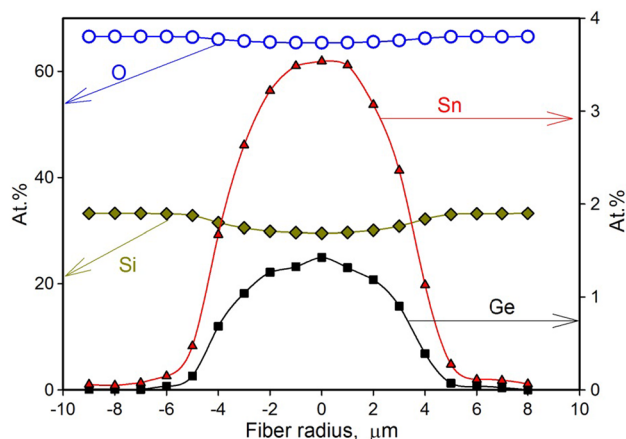


Fig. 7 Distribution of glass components across fiber core diameter

There is no sharp boarder between the tin-containing core and silica cladding due to mutual diffusion. No inclusions or any other defects are seen in the core. We have performed EDX microanalysis of the fiber across its core. The results are presented in Fig. 7.

Due to strong mutual diffusion of the core and cladding components, the concentrations of tin and germanium in the fiber core are much less than those in the charge. Nevertheless the ratio of tin to germanium remained similar to the ratio in the charge, and the shapes of tin and germanium distributions across the fiber look similar. It is interesting to note that silicon content even in the core center is about 20 times higher than that of germanium. Thus, the core consists of mostly silicate, and not germanate glass.

Using cleaved fiber pieces of 1 and 3 m in length, we have directly determined its numerical aperture as $\text{NA} = 0.486$. The refractive index of its core axis n_{core}

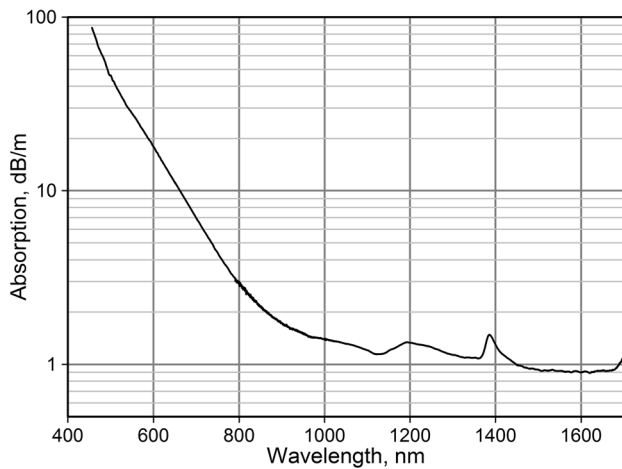


Fig. 8 Fiber losses spectrum

may be estimated as $n_{\text{core}} = 1.54$ from the formula $NA = \sqrt{n_{\text{core}}^2 - n_{\text{cladding}}^2}$ assuming $n_{\text{cladding}} = 1.48$.

The fiber losses spectrum measured by cleavage method in 5 m long fiber piece is presented in Fig. 8. One can see that the losses in $1.5 \div 1.6 \mu\text{m}$ range are less than 1 dB/m. We have detected no absorption peaks that could be associated with IR emission excitation. The absorption peak at $\sim 1.4 \mu\text{m}$ could be attributed to residual OH-groups in the glass.

Thus, fiber fabrication procedure starting from SnC_2O_4 – GeO_2 powders mixture in a silica tube resulted in multi-mode fiber with mostly silicate core composition. No traces of tin monoxide disproportionation into insoluble SnO_2 and metal Sn were detected during the fiber fabrication procedure.

5 Summary

$x\text{SnO} - (1-x)\text{GeO}_2$ glass samples were synthesized for a wide range of tin concentrations range $x = 0 \div 0.5$. In

contrast to tin silicate glasses, no evidence of SnO disproportionation during the synthesis took place. Clear glasses without SnO_2 and metal Sn inclusions were obtained in alumina and silica crucibles. All divalent tin-containing germanate glasses showed wideband photoluminescence peaking at about 1600 nm under $0.95 \mu\text{m}$ excitation. The photoluminescence intensity increases with tin content in the glass. Its e-fold decay time reached 440 μs at low tin concentration. Principal possibility to fabricate a fiber with divalent tin-containing core in a silica cladding was demonstrated using powder-in-tube method.

Acknowledgments The investigation was supported by RFBR Grant 14-02-00296 in the part of glass synthesis, by RFBR Grant 14-29-08168 in the part of fiber fabrication, and by the P1 Program of RAS Presidium in the part of spectral investigations. The authors are also thankful to S.V. Firstov for fiber losses measurements.

Compliance with ethical standards

Conflict of interest The authors declare that they have no conflict of interest.

References

1. I.A. Bufetov, M.A. Melkumov, S.V. Firstov, K.E. Riumkin, A.V. Shubin, V.F. Khopin, A.N. Guryanov, E.M. Dianov, *IEEE J. Sel. Top. Quantum Electron.* **20**, 0903815 (2014)
2. A.S. Zlenko, S.V. Firstov, K.E. Riumkin, V.F. Khopin, L.D. Iskhakova, S.L. Semjonov, I.A. Bufetov, E.M. Dianov, *Quantum Electron.* **42**, 310–314 (2012)
3. A.S. Zlenko, V.M. Mashinky, V.O. Sokolov, V.V. Koltashev, N.M. Karatun, L.D. Iskhakova, S.L. Semjonov, V.G. Plotnichenko, *J. Opt. Soc. Am. B* **20**, 675 (2016)
4. B.I. Denker, B.I. Galagan, L.D. Iskhakova, S.E. Sverchkov, E.M. Dianov, *Appl. Phys. B* **120**, 13 (2015)
5. D. Holland, M.E. Smith, I.J.F. Poplett, J.A. Johnson, M.F. Thomas, J. Bland, *J. Noncryst Solids* **293–295**, 175 (2001)